Analysis of Aharonov-Bohm effect due to time-dependent vector potentials

B. Lee, E. Yin, and T. K. Gustafson
Department of Electrical Engineering, University of California, Berkeley, California 94720

R. Chiao
Department of Physics, University of California, Berkeley, California 94720
(Received 12 November 1991)

We analyze and propose a method to detect the Aharonov-Bohm effect due to time-varying vector potentials, specifically those arising from a coherent light source. We show that the effect is feasible for use as a light-intensity detector. The quantum limit of detection is that of a single photon. Such a system would be a quantum-nondemolition measurement since no photon absorption occurs.

PACS number(s): 12.20.−m, 42.50.Wm, 03.65.Bz, 41.75.Fr

I. INTRODUCTION

Since the original paper by Aharonov and Bohm [1], numerous experiments [2–4] have detailed the phase change acquired by an electron propagating in the presence of electromagnetic potentials. The detection schemes have involved both free electrons and electrons in metallic rings. These researchers have been mainly interested in the nonlocality of the electromagnetic potentials. Therefore these experiments have involved only time-independent potentials, particularly vector potentials. In this paper we analyze the Aharonov-Bohm effect due to a time-dependent vector potential and consider the feasibility of experimentally observing this effect. Specifically, we suggest a method of detecting the electromagnetic potentials of a coherent light source, thereby detecting the beam intensity without actually absorbing the photons, and thus constituting a quantum-nondemolition experiment.

II. THEORY

Figure 1 illustrates the geometry typically used to observe the Aharonov-Bohm effect. A coherent electron beam which enters from the left is split around a magnetic flux, and is then recombined. When the flux inside the loop is varying with time, Maxwell's equations forbid a vanishing electromagnetic field on the loop itself in accordance with Faraday's law. However, even though the electromagnetic field will act on the electrons, the amplitude can be made small enough such that the phase change due to the potential will be the principal effect when the electrons are recombined.

Assuming cylindrical symmetry, we can approximate the situation with the geometry shown in Fig. 2, where we have taken the x axis to be that of the electron path. We then deal with the one-dimensional nonrelativistic Schrödinger equation for the electron, which is given by

$$\frac{1}{2m}\left[-i\hbar\frac{\partial}{\partial x}-\frac{e}{c}\mathbf{A}\right]^2\Psi+\Phi\Psi=i\hbar\frac{\partial\Psi}{\partial t} \tag{1}$$

where $\mathbf{A}$ and Φ are the vector and scalar potentials, respectively, and e, where e is negative, is the electron charge. Without any loss of generality, we can take the scalar potential to be zero everywhere.

It is convenient to use an inertial frame $x'=x-vt$ moving with the average phase velocity v of the electron. The phase velocity of the electron is half that of the group, or classical, velocity. In this frame the Schrödinger equation becomes

$$\frac{1}{2m}\left[-i\hbar\frac{\partial}{\partial x'}-\frac{e}{c}\mathbf{A}'\right]^2\Psi'+\Phi'\Psi'=i\hbar\frac{\partial\Psi'}{\partial t'} \tag{2}$$

where $\mathbf{A}'$ and Φ' are the vector and scalar potentials in the moving frame, and $t'=t$ as we are only dealing with

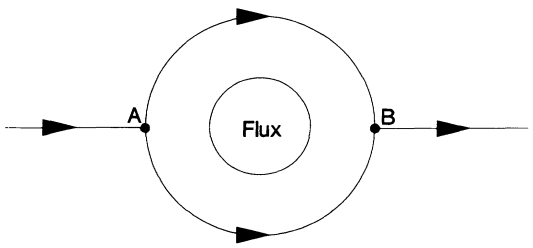

FIG. 1. Schematic illustration of the Aharonov-Bohm phase experiment.

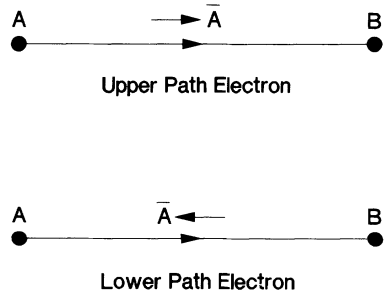

FIG. 2. Simplified geometry of electron paths using cylindrical symmetry.

the nonrelativistic case. The electron wave function $\Psi'(x',t')$ in the moving frame is related to the electron wave function $\Psi(x,t)$ in the laboratory frame by [5]

$$\Psi'(x',t')=\Psi(x,t)\exp\left[-i\frac{mv}{\hbar}x+i\frac{mv^2}{2\hbar}t\right] . \tag{3}$$

The potentials $\mathbf{A}'$ and Φ' are related to the potential $\mathbf{A}$ (Φ is taken to be zero) by [6]

$$\begin{aligned}&\mathbf{A}'(t')=\mathbf{A}(t) ,\\ &\Phi'(t')=-\frac{ev}{c}\mathbf{A}(t) .\end{aligned} \tag{4}$$

The interference which arises when the electrons recombine on the right side of the loop is directly related to the difference of the wave-function phases associated with the upper electron path and the lower electron path, respectively. Since the phase in Eq. (3) is the same for both the upper and lower path electrons, it has no physical effect. We need therefore only consider Eq. (2). We write the solution of this equation in the form

$$\begin{aligned}\Psi'(x',t')&=\Psi'_a(x',t')\exp\left[-\frac{i}{\hbar}\int_0^{t'}\Phi' dt'\right]\\ &=\Psi'_a(x',t')\exp\left[\frac{ie}{\hbar c}v\int_0^{t'}\mathbf{A}'dt'\right]\end{aligned} \tag{5}$$

where

$$\frac{1}{2m}\left[-i\hbar\frac{\partial}{\partial x'}-\frac{e}{c}\mathbf{A}'\right]^2\Psi'_a=i\hbar\frac{\partial\Psi'_a}{\partial t'} . \tag{6}$$

Ψ'_a in turn can be written as

$$\Psi'_a(x',t')=\Psi'_b(x',t')\exp\left[\frac{ie}{\hbar c}\int_0^{x'}\mathbf{A}'\cdot d\mathbf{x}'\right] \tag{7}$$

where Ψ'_b satisfies the following partial differential equation:

$$-\frac{\hbar^2}{2m}\frac{\partial^2\Psi'_b}{\partial x'^2}+\frac{e}{c}\left[\int_0^{x'}\frac{\partial\mathbf{A}'}{\partial t'}\cdot d\mathbf{x}'\right]\Psi'_b=i\hbar\frac{\partial\Psi'_b}{\partial t'} . \tag{8}$$

The second term on the left-hand side of Eq. (8) can be modeled as a scalar potential term due to Faraday's law as in

$$\begin{aligned}\frac{e}{c}\int_0^{x'}\frac{\partial\mathbf{A}'}{\partial t'}\cdot d\mathbf{x}'&=\frac{e}{c}\frac{\partial}{\partial t'}\int_0^{x'}\mathbf{A}'\cdot d\mathbf{x}'\\ &=-e\left[-\frac{\partial}{\partial t'}\frac{F}{c}\right]\\ &=-e\mathscr{E}\end{aligned} \tag{9}$$

where F is the flux and $\mathscr{E}$ the electromotive force. Therefore, Eq. (8) can be considered to be the wave equation due to only Faraday's law. Substituting Eq. (7) into Eq. (5), the wave function can be separated into two terms:

$$\Psi'(x',t')=\Psi'_b(x',t')\times\exp\left[\frac{ie}{\hbar c}\left[\int_0^{x'}\mathbf{A}'\cdot d\mathbf{x}'+v\int_0^{t'}\mathbf{A}'dt'\right]\right] \tag{10}$$

where Ψ'_b contains the effects of Faraday's, or Maxwell's, law, and the phase factor

$$\exp\left[\frac{ie}{\hbar c}\left[\int_0^{x'}\mathbf{A}'\cdot\mathbf{x}'+v\int_0^{t'}\mathbf{A}'dt'\right]\right]$$

comes from the requirement of gauge invariance of the Schrödinger equation, or equivalently, the Aharonov-Bohm effect. Because of Faraday's law, the function $\Psi'_b(x',t')$ is different from the free particle wave function $\Psi'_0(x',t')$. However, the difference between $\Psi'_b(x',t')$ and $\Psi'_0(x',t')$ is negligible for the case of particular interest, that of the detection of optical signals (see Appendix A).

We note in Eq. (10) that there are two contributions to the Aharonov-Bohm phase. The first, $\exp[(ie/\hbar c)v\int_0^{t'}\mathbf{A}'dt']=\exp[(ie/\hbar c)v\int_0^{t}\mathbf{A}\,dt]$, is that due to the average speed of the electron. This corresponds to the usual dc Aharonov-Bohm effect. A second contribution, $\exp[(ie/\hbar c)\int_0^{x'}\mathbf{A}'\cdot d\mathbf{x}']$, arises from the velocity modulation which is a consequence of Faraday's law. This can be estimated from Newton's law. For the present case, the second term is negligible (or zero if $x'=0$ when the electrons recombine) since the electron oscillation is small for fields at optical frequencies. The phase factor in Eq. (10) can also be derived using Feynman's path-integral method (see Appendix B).

Since electrons move slowly across the loop compared with optical frequencies, the vector potential oscillates many times before the electrons reach the other end of the loop. Only the last uncanceled cycle contributes to the final change. For sinusoidally varying vector potentials, the interference at the end of the loop is proportional to the quantity

$$\begin{aligned}P&\equiv\frac{1}{4}\left|\exp\left[\frac{ie}{\hbar c}v\int_0^t\mathbf{A}\,dt\right]+\exp\left[\frac{ie}{\hbar c}v\int_0^t(-\mathbf{A})dt\right]\right|^2\\ &=\frac{1}{4}\left|\exp\left[-\frac{ie}{\hbar c}v\int_0^t\mathbf{A}\,dt\right]\right|^2\left|\exp\left[\frac{2ie}{\hbar c}v\int_0^t\mathbf{A}\,dt\right]+1\right|^2\\ &=\frac{1}{4}\left|\exp\left[\frac{2ie}{\hbar c}vA_0\int_0^t\cos(\omega t)dt\right]+1\right|^2=\frac{1}{4}\left|\exp\left[\frac{2ie}{\hbar c}vA_0\frac{\sin(\omega t)}{\omega}\right]+1\right|^2\\ &=\frac{1}{2}\left[1+\cos\left[\frac{2evA_0}{\hbar c\omega}\sin\omega t\right]\right]=\frac{1}{2}\left[1+\sum_{n=-\infty}^{\infty}J_n\left[\frac{2evA_0}{\hbar c\omega}\right]\cos(n\omega t)\right] ,\end{aligned} \tag{11}$$

where $\mathbf{A}=A_0\cos(\omega t)$ is assumed and $J_n(\ )$'s are Bessel functions. The high optical frequencies can easily be filtered out in the detection circuit. Therefore the electronic conductivity will be proportional to only the dc term, i.e.,

$$P' \equiv \frac{1}{2}\left[1+J_0\left[\frac{2ev A_0}{\hbar c\omega}\right]\right] . \tag{12}$$

This equation is valid even for electrons traveling at relativistic speeds since the phase change in Eq. (10) is valid for this case. Figure 3 shows the graph of the dc term P' versus the amplitude of the vector potential A_0.

III. QUANTUM LIMIT OF DETECTION

The quantum limit of detection for this system is that of a single photon. This can be derived using a half wavelength as the interaction length, so that there is no excess cancellation of phase. We may approximate the interference at the end of the loop as the difference between the phase changes of the upper and lower path electrons. For an enclosed flux of $\frac{1}{2}\Phi_0$, where Φ_0 is a single flux quantum h/e in mks units, which results in a π phase shift, one obtains

$$2A_0\frac{\lambda}{2}=\frac{h}{2e} . \tag{13}$$

This corresponds to a beam intensity of

$$I=\frac{h^2\omega^2}{4Z_0e^2\lambda^2} \tag{14}$$

where

$$Z_0=\left[\frac{\mu_0}{\varepsilon_0}\right]^{1/2}=377\ \Omega .$$

For a beam focused down within the interaction length, and assuming an infinite bandwidth detector, we obtain the energy E for a half cycle of light

$$E=nh\omega/2\pi=\frac{h^2\omega}{8Z_0e^2} \tag{15}$$

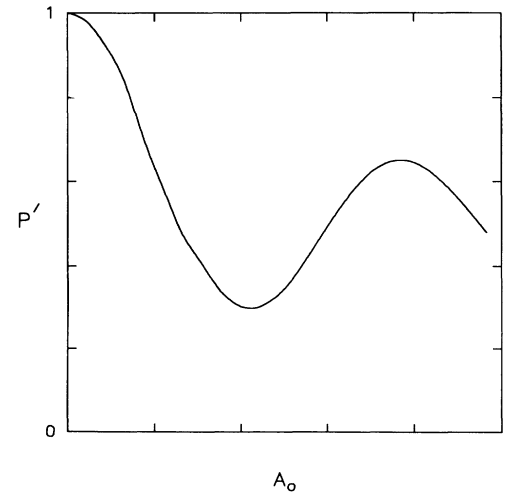

FIG. 3. dc electronic conductivity vs vector potential.

where n is the number of photons. This reduces to

$$n=\frac{\pi h}{4Z_0e^2}=\frac{\pi}{8\alpha} ,$$
$$n=54 \text{ photons} , \tag{16}$$

where $\alpha\approx\frac{1}{137}$ is the fine-structure constant. For a single photon passing through the system, the enclosed flux is reduced by a factor of $\sqrt{54}$. Therefore a single photon will cause a phase change of $\pi/\sqrt{54}$, corresponding to a 4.5% change in conductivity, which is within the limits of detection. This agrees with the prediction of a 4.6% suppression of critical current in a Mercereau ring interferometer due to a single photon deduced by one of the authors [7]. We therefore conclude that the quantum limit of this system is the detection of a single photon.

IV. EXPERIMENTAL SETUP

We now propose a method to detect the Aharonov-Bohm effect due to a coherent light source. One possible method to obtain a magnetic flux within an electron loop is to use total internal reflection off a crystal surface. We may therefore observe the evanescent magnetic fields emanating from the other side of the crystal. Accordingly, the coherent electron beam must be very close to the surface of the crystal. An ideal configuration would be to evaporate a small metal ring on the crystal surface and observe the electron interference by simply measuring the conductivity. However, the maximum electron velocity in a metal, which is limited roughly by the Fermi velocity, is too low to observe sufficient interference [from Eq. (12)]. Therefore the electron loop must consist of free electrons traveling at high speeds. Due to the large focusing lengths required when dealing with electron optics, the path length necessary to recombine the electron beams may be too long to preserve coherence. Therefore we propose the system shown in Fig. 4. Two slits, far enough apart to accommodate a focused beam between them, are located near the surface of the crystal. An electron beam illuminates the slits, and the resulting electron diffraction pattern is measured. The laser beam is focused within the two electron trajectories, causing a shift in the diffraction peaks due to the Aharonov-Bohm effect. However, as the peak shifts are oscillating at optical frequencies, the most convenient method of detection is that of measuring the increase in central peak broadening.

For the diffraction experiment as shown in Fig. 4, the relative change in the central peak diffraction angle is given by (see Appendix D)

$$\frac{\Delta\theta}{\theta_0}=\frac{4ev A_0}{\pi\hbar c\omega} \tag{17}$$

where $2\Delta\theta$ is the change in the central peak angle due to the vector potential, and $2\theta_0$ is the central peak angle when no electromagnetic field is present inside the loop. From Eq. (17), we see that the relative change in the central peak diffraction angle is dependent on the optical frequency and beam intensity. A change in either of these parameters will result in a change in the electron diffraction pattern. We see an immediate application for

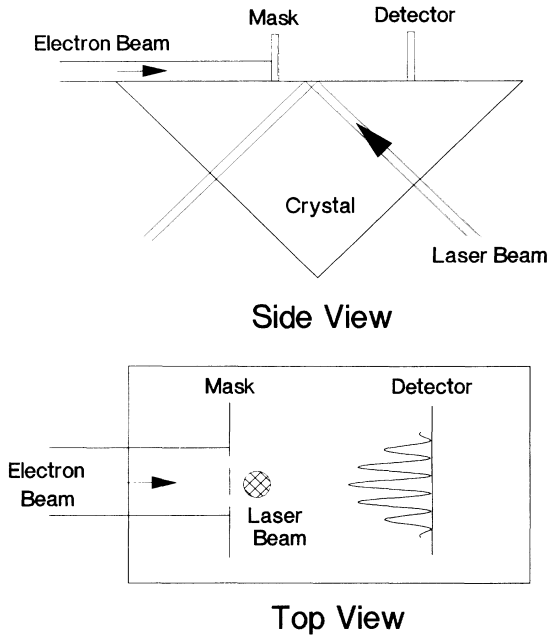

FIG. 4. Possible experimental setup for the observation of the vector potential of coherent light using electron interference experiment.

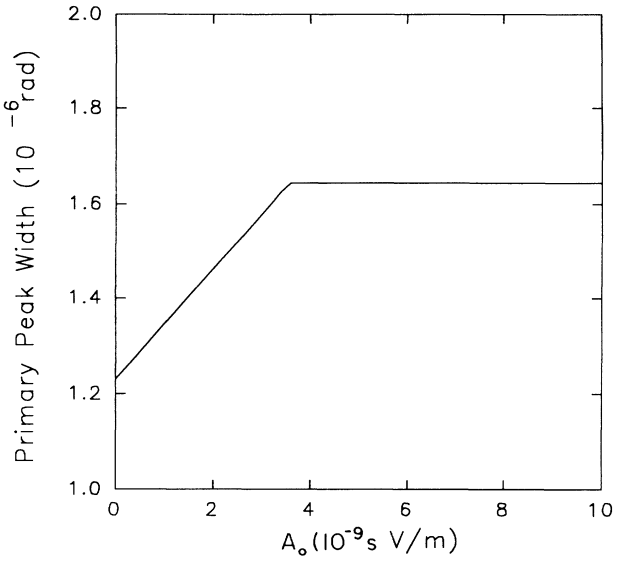

FIG. 5. Width in primary interference peak vector potential.

this system as a light intensity detector. The system is particularly interesting in that there are only virtual exchanges of energy from the photons to the electrons and vice versa. The photons are not absorbed as in most photodetectors, but merely diverted. Therefore this constitutes a quantum-nondemolition measurement. Figure 5 shows a plot of the primary peak width versus $\mathbf{A}_0$ for $v=3\times10^7$ m/s (voltage of 10 kV), and $\omega=10^{15}$ rad/s. The primary peak has a full width at half maximum of 1.23×10^{-6} rad for $d=5$ μm for no applied electromagnetic potential. We see, for example, that a change of $\mathbf{A}_0$ from zero to 1.7×10^{-9} s V/m, or equivalently a beam intensity of 7.9×10^5 W/cm^2, will result in a 10% increase in the central peak width. For a laser spot size of 3 μm, this intensity corresponds to a power of 0.056 W. Therefore this effect should be detectable with a reasonably powered laser. The width increase is shown to saturate due to the proximity of the next interference peak. Using lower-frequency fields will enhance the sensitivity of the system.

V. CONCLUSIONS

In conclusion, we have analyzed the Aharonov-Bohm effect for time-dependent electromagnetic potentials and have shown that this effect should be observable in an electron interference experiment. For a known beam frequency and electron energy, this can be used as a light intensity detector. Since the photons are not absorbed, this constitutes a quantum-nondemolition measurement. It is also possible that the resulting photons will be in a squeezed number state as the photon number uncertainty will be decreased. The quantum limit of such a system is the detection of a single photon.

ACKNOWLEDGMENT

This work was supported in part by the U.S. Air Force Office of Scientific Research under Grant No. 1-442427-22514.

APPENDIX A

For $A'(x',t')=A_0\cos\omega t'$, Eq. (8) becomes

$$-\frac{\hbar^2}{2m}\frac{\partial^2\Psi_b'}{\partial x'^2}-\frac{e\omega}{c}A_0x'\sin(\omega t')\Psi_b'=i\hbar\frac{\partial\Psi_b'}{\partial t'}\ . \quad \text{(A1)}$$

Using a classical approach, we can estimate the maximum displacement of an oscillating electron by Newton's law:

$$x'_{\max}=\frac{eA_0}{cm\omega}\ . \quad \text{(A2)}$$

Substituting the free electron solution $\Psi_0'(x',t')=e^{ikx'-i\omega_0t'}$ into the left-hand side of Eq. (A1) and using Eq. (A2), we can estimate the ratio of the first term to the second to be

$$\frac{\hbar^2k^2/2m}{e^2A_0^2/c^2m}\ .$$

For typical values of $v=10^6$ m/s and $A_0=5\times10^{-9}$ s V/m, this ratio is equal to 6×10^{22}. Therefore we see that $\Psi_0'(x',t')=e^{ikx'-i\omega_0t'}$ is a good approximation for the solution of Eq. (A1) where $\omega_0=\hbar k^2/2m$.

APPENDIX B

According to Feynman's path-integral method [8,9], the wave function $\Psi(t)$ is obtained from the incident wave function $\Psi(0,0)$ by the integral

$$\Psi(x,t)=\int d^3x \sum_{[x_0(t_0)]} \exp\left[\frac{i}{\hbar}\int_0^t\left[\frac{1}{2}mv_0^2+\frac{e}{c}\mathbf{A}(x_0,t_0)v_0\right]dt_0\right]\Psi(0,0)$$

where the summation is over all possible space-time paths (x_0,t_0) with the boundary conditions given by $x(0)=0$ and $x(t)$. The classical path which minimizes the action of the path integral is the path which provides the major contribution to the wave function $\Psi(x,t)$. Therefore

$$\Psi(x,t)\approx\Psi(0,0)\exp\left[\frac{im}{2\hbar}\int_0^t v^2(t)dt\right]\exp\left[\frac{ie}{\hbar c}\int_0^x \mathbf{A}(x(t),t)\cdot d\mathbf{x}(t)\right]$$

where $x(t)$ is the classical path. Here, the first exponential on the right-hand side can be written as

$$\exp\left[\frac{im}{2\hbar}\int_0^t v^2(t)dt\right]=\exp\left[\frac{im}{2\hbar}\int_0^t[v_{\rm dc}(t)+v_{\rm ac}(t)]^2dt\right]$$

$$=\exp\left[\frac{im}{2\hbar}\int_0^t[v_{\rm dc}^2(t)+v_{\rm ac}^2(t)]dt\right]\exp\left[\frac{im}{\hbar}\int_0^t v_{\rm dc}(t)v_{\rm ac}(t)dt\right]$$

where the first factor is the same for upper and lower path electrons while the second factor is different because the ac velocities are opposite in direction. However, this Faraday effect can be neglected when compared with the phase change

$$\exp\left[\frac{ie}{\hbar c}\int_0^x \mathbf{A}(x(t),t)\cdot d\mathbf{x}(t)\right]=\exp\left[\frac{ie}{\hbar c}\int_0^t \mathbf{A}(x(t),t)\cdot\frac{d\mathbf{x}(t)}{dt}dt\right]$$

$$=\exp\left[\frac{ie}{\hbar c}\int_0^{t'} \mathbf{A}'(x'(t'),t')\cdot\frac{d[x'(t')+vt']}{dt'}dt'\right]$$

$$=\exp\left[\frac{ie}{\hbar c}\int_0^{t'} \mathbf{A}'(x'(t'),t')\cdot\frac{d\mathbf{x}'(t')}{dt'}dt'+\frac{ie}{\hbar c}v\int_0^{t'}\mathbf{A}'(x'(t'),t')dt'\right]$$

$$=\exp\left[\frac{ie}{\hbar c}\int_0^{x'} \mathbf{A}'(x'(t'),t')\cdot d\mathbf{x}'(t')+\frac{ie}{\hbar c}v\int_0^{t'}\mathbf{A}'(x'(t'),t')dt'\right],$$

which is integrated over the classical path and in accordance with the phase factor in Eq. (10).

APPENDIX C

In our case, we can start with the Klein-Gordon equation [10]

$$\left[-\frac{\hbar}{i}\frac{\partial}{\partial t}-e\Phi\right]^2\Psi\left[\frac{\hbar}{i}\frac{\partial}{\partial x}-\frac{e}{c}\mathbf{A}\right]^2\Psi=c^4m^2\Psi\ .$$

In an inertial frame moving with the average phase velocity of the electrons, $v\hat{x}$, the equation becomes

$$\left[-\frac{\hbar}{i}\frac{\partial}{\partial t'}-e\Phi'\right]^2\Psi'-\left[\frac{\hbar}{i}\frac{\partial}{\partial x'}-\frac{e}{c}\mathbf{A}'\right]=c^4m^2\Psi'$$

where

$$x'=\gamma(x-vt),\quad t=\gamma\left[t-\frac{v}{c^2}x\right],$$

$$\mathbf{A}'=\gamma\mathbf{A},\quad \Phi'=-\gamma\frac{v}{c}\mathbf{A},$$

$$\gamma=\frac{1}{(1-v^2/c^2)^{1/2}}\ .$$

The solution is

$$\Psi'=\Psi_b'\exp\left[-\frac{ie}{\hbar}\int_0^{t'}\Phi'dt'\right]\exp\left[\frac{ie}{\hbar c}\int_{x_0}^{x'}\mathbf{A}'\cdot d\mathbf{x}'\right]$$

where Ψ_b' satisfies

$$\left[-\frac{\hbar}{i}\right]^2\frac{\partial^2\Psi_b'}{\partial t'^2}+\frac{2e\hbar}{ic}\left[\int_{x_0}^{x'}\frac{\partial \mathbf{A}'}{\partial t'}dx'\right]\frac{\partial\Psi_b'}{\partial t'}+\frac{e\hbar}{ic}\left[\int_{x_0'}^{x'}\frac{\partial^2\mathbf{A}'}{\partial t'^2}dx'\right]\Psi_b'$$
$$+\frac{e^2}{c^2}\left[\int_{x_0'}^{x'}\frac{\partial\mathbf{A}'}{\partial t'}dx'\right]^2\Psi_b'-\left[\frac{\hbar}{i}\right]^2\frac{\partial^2\Psi_b'}{\partial x'^2}=c^4m^2\Psi_b' .$$

Similar to the nonrelativistic case, the difference of Ψ_b' from the free-field wave function Ψ_0' is small compared to the effect of the phase factor. The phase factor is given by

$$\exp\left[-\frac{ie}{\hbar}\int_0^{t'}\mathbf{A}'dt'\right]\exp\left[\frac{ie}{\hbar c}\int_{x_0'}^{x'}\mathbf{A}'\cdot d\mathbf{x}'\right]$$
$$=\exp\left[\frac{ie}{\hbar c}v\gamma\int_0^{t'}\mathbf{A}\,dt'\right]\exp\left[\frac{ie}{\hbar c}\gamma\int_{x_0'}^{x'}\mathbf{A}\cdot d\mathbf{x}'\right]$$
$$=\exp\left[\frac{ie}{\hbar c}\gamma^2v\int_0^t\mathbf{A}\,dt-\frac{ie}{\hbar c}\gamma^2\frac{v^2}{c^2}\int_{x_0}^{x}\mathbf{A}\cdot d\mathbf{x}\right]\exp\left[\frac{ie}{\hbar c}\gamma^2\int_{x_0}^{x}\mathbf{A}\cdot d\mathbf{x}-\frac{ie}{\hbar c}\gamma^2v\int_0^t\mathbf{A}\,dt\right]$$
$$=\exp\left[\frac{ie}{\hbar c}\gamma^2\left[1-\frac{v^2}{c^2}\right]\int_{x_0}^{x}\mathbf{A}\cdot d\mathbf{x}\right]=\exp\left[\frac{ie}{\hbar c}\int_{x_0}^{x}\mathbf{A}\cdot d\mathbf{x}\right]=\exp\left[\frac{ie}{\hbar c}\int_0^t\mathbf{A}\cdot\frac{d\mathbf{x}}{dt}dt\right]=\exp\left[\frac{ie}{\hbar c}v\int_0^t\mathbf{A}\,dt\right] .$$

This phase factor is the same as that of the nonrelativistic case in Eq. (10).

APPENDIX D

For the electron diffraction experiment as shown in Fig. 4, Eq. (11) can be modified as the following:

$$P=\frac{1}{4}\left|\exp\left[\frac{ie}{\hbar c}v\int_0^t\mathbf{A}\,dt+i\omega_e t\right]+\exp\left[\frac{ie}{\hbar c}v\int_{-\tau}^{t}(-\mathbf{A})dt+i\omega_e(t+\tau)\right]\right|^2$$
$$=\frac{1}{4}\left|\exp\left[-\frac{ie}{\hbar c}v\int_{-\tau}^{t}\mathbf{A}\,dt+i\omega_e(t+\tau)\right]\right|^2\left|\exp\left[\frac{i2e}{\hbar c}v\int_0^t\mathbf{A}\,dt+\frac{ie}{\hbar c}v\int_{-\tau}^{0}\mathbf{A}\,dt-i\omega_e\tau\right]+1\right|^2$$
$$=\frac{1}{2}\left[1+\cos\left[\frac{2ev}{\hbar c}\int_0^t\mathbf{A}\,dt+\frac{ev}{\hbar c}\int_{-\tau}^{0}\mathbf{A}\,dt-\omega_e\tau\right]\right]$$
$$=\frac{1}{2}\left[1+\cos\left[\frac{2evA_0}{\hbar c\omega}\sin(\omega t)+\frac{evA_0}{\hbar c\omega}\sin(\omega\tau)-\omega_e\tau\right]\right] \qquad \text{(D1)}$$

where ω_e is the angular frequency of an electron wave, and τ is the difference between the time necessary for the electron leaving the first slit and the electron leaving the second slit to reach the specified position at the screen. If we use a detection scheme which records the electron accumulation at each position on the screen, the condition for the primary peak half maximum to occur is given by

$$\omega_e\tau-\left[\frac{2evA_0}{\hbar c\omega}\sin(\omega t)+\frac{evA_0}{\hbar c\omega}\sin(\omega\tau)\right]_{\max}=\frac{\pi}{2} \qquad \text{(D2)}$$

because the second term in Eq. (D2) is always smaller than the first term. Because $\omega\tau$ is much smaller than unity in our experiment, we can approximate Eq. (D2) by

$$\omega_2\tau-\frac{2evA_0}{\hbar c\omega}\approx\frac{\pi}{2} .$$

The time difference τ is related to the path difference by

$$\tau\approx\frac{d\sin\theta}{v}\approx\frac{d\theta}{v}$$

where d is the distance between slit A and slit B, θ is the diffraction angle, and v is the electron phase velocity. Therefore we can deduce the half angle θ of the primary peak to be

$$\theta=\frac{\pi v}{2\omega_e d}+\frac{2ev^2A_0}{\hbar c\omega\omega_e d} ,$$

while the half angle θ_0 of the primary peak width when no electromagnetic field is applied is given by

$$\theta_0=\frac{\pi v}{2\omega_e d}=\frac{\lambda_e}{4d} .$$

Therefore we deduce the relative angular increase in the primary peak width to be

$$\frac{\Delta\theta}{\theta_0}\equiv\frac{\theta-\theta_0}{\theta_0}=\frac{4evA_0}{\pi\hbar c\omega} .$$

[1] Y. Aharonov and D. Bohm, Phys. Rev. **115**, 485 (1959).
[2] R. Chambers, Phys. Rev. Lett. **5**, 3 (1960).
[3] R. Webb, S. Washburn, C. Umbach, and R. Laibowitz, Phys. Rev. Lett. **54**, 2696 (1985).
[4] V. Chandarasekhar, M. Brooks, S. Wind, and D. Prober, Phys. Rev. Lett. **55**, 1610 (1985).
[5] This is the Galilean transformation of a wave function for the potentials transformed as in Eq. (4). The Galilean transformation of a wave function in the case of a zero vector potential can be found in J. D. Jackson, *Classical Electrodynamics,* 2nd ed. (Wiley, New York, 1975), p. 505.
[6] This transformation of potentials comes from the expansion of Lorentz transformed potentials up to the first order in v/c. Relativistic transformations can be found in Appendix C and in J. D. Jackson, *Classical Electrodynamics,* 2nd ed. (Wiley, New York, 1975), p. 552.
[7] R. Chiao, Phys. Lett. **33A**, 177 (1970).
[8] R. P. Feynman, Rev. Mod. Phys. **20**, 367 (1948).
[9] T. Troudet, Phys. Lett. **111A**, 274 (1985).
[10] See, for example J. J. Sakurai, *Advanced Quantum Mechanics* (Addison-Wesley, New York, 1967), p. 7.